
VPNet: Variable Projection Networks

Péter Kovács^{1,3}, Gergő Bognár^{1,3}, Christian Huber², Mario Huemer¹,

¹Institute of Signal Processing, Johannes Kepler University Linz, 4040 Linz, Austria

³Department of Numerical Analysis, Eötvös Loránd University, 1117 Budapest, Hungary

²Silicon Austria Labs GmbH, 4040 Linz, Austria

{peter.kovacs, gergoe.bognar, mario.huemer}@jku.at
christian.huber@silicon-austria.com

Abstract

In this paper, we introduce VPNet, a novel model-driven neural network architecture based on variable projections (VP). The application of VP operators in neural networks implies learnable features, interpretable parameters, and compact network structures. This paper discusses the motivation and mathematical background of VPNet as well as experiments. The concept was evaluated in the context of signal processing. We performed classification tasks on a synthetic dataset, and real electrocardiogram (ECG) signals. Compared to fully-connected and 1D convolutional networks, VPNet features fast learning ability and good accuracy at a low computational cost in both of the training and inference. Based on the promising results and mentioned advantages, we expect broader impact in signal processing, including classification, regression, and even clustering problems.

1 Introduction

Till the last decade, the field of signal processing was dominated by conventional model-based algorithms, which rely on mathematical and physical models of the real world. Inherently, they are interpretable and often incorporate domain knowledge such as statistical assumptions, smoothness, structure of the model space, or origin of the noise. However, this approach becomes mathematically intractable in case of complex problems. Machine learning (ML) provides an alternative to solve this challenge by building up data-driven mathematical models. Especially, neural networks (NNs) and supervised learning provide a proper framework for various signal processing problems [1]. In the following, we briefly review a few recent trends that serve as motivations for the proposed variable projection network (VPNet).

A traditional ML approach is the decomposition of the problem into separate feature extraction and learning steps [2]. In this case, the data is preprocessed in order to extract static features based on the given domain knowledge. These features are forwarded to the input of conventional ML algorithms. Although the dimension of the original data is significantly reduced in the first step, these handcrafted features are usually suboptimal with respect to the whole learning process [3]. Deep learning provides alternatives to the traditional approach overcoming some of its drawbacks [1]. The usage of more hidden layers in deep neural networks (DNNs) increased the learning abilities of NNs [4]. This enables DNNs to use the first layers for feature extraction and subsequent layers to perform operation on these learned features. Convolutional neural networks (CNNs) are special, optionally deep architectures that are the leading ML methods in 2D and 3D image processing and computer vision [5–8]. Here, the built-in feature extraction layers perform multiple convolutional filtering and dimension reduction (pooling) steps. Despite their advantages, DNNs and CNNs still raise several concerns. The improved efficiency comes at the cost of higher computational complexity and numerical difficulties in the training process (see e.g. overfitting and divergence). Due to the large number of nonlinear connections between the model parameters, DNN and CNN approaches

can be considered as black-box methods, where the parameters have no physical meaning and are difficult or impossible to interpret. Additionally, a huge amount of labeled data is required to train these networks, which is problematic to collect in many applications such as telecommunication [9], and biomedical engineering [10, 11].

Model-driven NN constructions such as deep unfolding [12] and Wiener-, Hammerstein-type NNs [13] are attempted to resolve the aforementioned drawbacks of DNNs. The former approach unfolds the iterations of classical model-based algorithms into layer-wise NN structures whose parameters are optimized based on the training data. This way the resulting NN retains the powerful learning ability of DNNs, inherits expert knowledge, and reduces the size of the training data [9]. Wiener- [14], and Hammerstein-type NNs [13] are alternatives to fuse the best properties of model based methods and deep learning techniques. These networks comprise cascades of static nonlinear elements and dynamic linear blocks, representing NNs and linear time-invariant (LTI) systems, respectively. Recently, these methods have shown great potential in many fields such as system identification [13], control engineering [14], sparse approximation theory [15, 16], and telecommunication [17, 18].

Despite the popularity of deep learning and the advances of model-driven NNs, traditional ML algorithms still dominate in many 1D signal processing tasks [19], especially in biomedical signal classifications such as electroencephalogram (EEG), electromyogram (EMG), and ECG classification. The main reason behind that lies in the nature of clinical applications, where both accuracy and explainability are important. This cannot be guaranteed by the previously mentioned model-driven NN approaches, since they do not extract medically interpretable features. This is where the VPNet comes into picture. The theory of variable projection (VP) provides a framework to solve nonlinear least squares problems, whose parameters can be separated into linear and nonlinear ones. In many fields of signal processing, there is a large number of linear parameters, which are driven by a smaller number of nonlinear variables (see Eq. (3)). For example, signal compression, representation, and feature extraction algorithms are often based on linear coefficients of some transformation such as Fourier transform, wavelet transform, or eigenvalue decomposition. The corresponding nonlinear parameters have a physical meaning, e.g. they can be described by frequencies, properties of the window function, free parameters of the wavelets, and so on [20].

The VPNet was designed to merge the expert knowledge used by traditional model-based approaches with the learning abilities of NNs. The theoretical background, the general formulation of VPNet, and the corresponding backpropagation algorithm will be discussed in Section 2. Further, we will perform multiple experiments to evaluate and compare the performance of VPNet to other NNs in Section 3. Finally, Section 4 is a summary of conclusions and expected broader impact of our research.

2 Variable Projection Networks

2.1 Variable Projections

Variable Projection (VP) [21] provides a framework to address nonlinear modeling problems of the form

$$x \approx \hat{x} = \sum_{k=0}^{n-1} c_k \Phi_k(\theta) = \Phi(\theta)c, \quad (1)$$

where $x \in \mathbb{R}^m$ and $\Phi_k \in \mathbb{R}^m$ denote the input data to be approximated, and a parametric function system, respectively. The symbol $\Phi(\theta)$ will refer to both the function system itself, and to a matrix of size $\mathbb{R}^{m \times n}$. The linear parameters $c \in \mathbb{R}^n$ and the nonlinear parameters $\theta \in \mathbb{R}^p$ of function system Φ are separated as above. The least squares fit of this problem means the minimization of the nonlinear functional

$$r(c, \theta) := \|x - \Phi(\theta)c\|_2^2.$$

Without nonlinear parameters (i.e. if θ is fixed), the model is linear in the coefficients c . The minimization of r with respect to c leads to the well-known linear least squares approximation. We remark that it is actually the best approximation problem in Hilbert spaces. The optimal solution can be expressed by means of Fourier coefficients and orthogonal projection operators $\mathcal{P}_{\Phi(\theta)}$:

$$c = \Phi^+(\theta)x, \quad \hat{x} = \mathcal{P}_{\Phi(\theta)}x = \Phi(\theta)\Phi^+(\theta)x, \quad (2)$$

where $\Phi^+(\theta)$ denotes the Moore–Penrose pseudoinverse of matrix $\Phi(\theta)$. The concept is strongly related to the mathematical transformation methods, such as Fourier and wavelet transforms, that

can be interpreted as an orthogonal projection by a given function system with a predefined θ . In a practical point of view, the coefficients c can be interpreted as features extracted by VP, and \hat{x} is a result of a lowpass filtering and dimension reduction. The minimization of r in the general case can be decomposed into the minimization by the nonlinear parameters θ , while the linear parameters c are computed by the orthogonal projection. Thus, the minimization of r is equivalent to the minimization of the following VP functional (see e.g. Theorem 2.1 in [21]):

$$r_2(\theta) := \|x - \Phi(\theta)\Phi^+(\theta)x\|_2^2. \quad (3)$$

In [21], formulae and a gradient iteration is provided for the numerical optimization of r_2 . Mathematically, VP is a formalization for adaptive orthogonal transformations that allows filtering and feature extraction by means of parametric function systems. On the other hand, if a nonlinear optimization problem can be separated to linear and nonlinear parameters, VP may act as a solver, leading to several other applications [22].

VP comes into picture with ML as a feature extraction method, and as a modeling technique for the training procedure [23]. The latter work proposes VP as an optimization method for a given class of feedforward NNs. There, the whole network is modeled with VP, and the VP optimization method of [21] is utilized as an alternative to stochastic gradient methods. This methodology is however limited to NNs with only one hidden layer. Here, we propose VPNet by a completely different and novel aspect, based on the feature extraction ability of VP. Previous results show that several biomedical signal processing problems can be addressed efficiently with variable projection by means of adaptive rational and Hermite functions, as well as B-splines [20, 24]. VP features were particularly utilized for ECG and EEG representation, compression, classification, and segmentation [25–32]. The results show that VP provides a very compact, yet morphologically accurate representation of signals with respect to the target problem. Additionally, the nonlinear parameters themselves carry direct morphological information about the signals, and they are usually interpretable in a natural way.

2.2 VPNet

Motivated by the aspects in Section 1, we introduce the VPNet architecture. The key idea is to create a network that combines the representation abilities of VP and the prediction abilities of NNs in form of a joint model. The basic VPNet architecture is a feedforward NN, where the first layer(s) applies a VP operator that is forwarded to a fully-connected, potentially deep NN (see Fig. 1). The construction is similar to the CNNs in the sense that the first layer(s) of the network can be interpreted as a built-in feature extraction method. Here we note, that more complex VPNet architectures are also possible, e.g. on the model of U-Net [8] and AutoEncoder [33], which will be investigated in our future work.

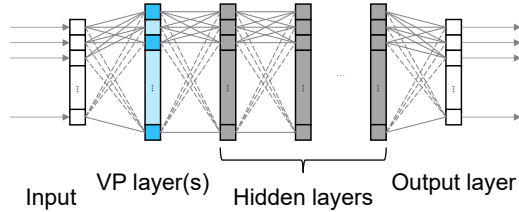


Figure 1: VPNet architecture.

The VP layer we propose has two possible behaviours, depending on its target application. It either performs a filtering of the form

$$f^{(\text{vp})}(x) := \Phi(\theta)\Phi^+(\theta)x = \hat{x} \quad (x \in \mathbb{R}^m), \quad (4)$$

or a feature extraction of the form

$$f^{(\text{vp})}(x) := \Phi^+(\theta)x = c \quad (x \in \mathbb{R}^m), \quad (5)$$

where $\theta \in \mathbb{R}^p$ denotes the nonlinear system parameters of the given function system Φ , as defined above. These VP operators refer to the orthogonal projection and the general Fourier coefficients of the input x by means of the parametric system $\Phi(\theta)$, as in Eq. (2). The filter method may fit better for regression problems, while the feature extraction is suitable for classification problems. The nonlinear system parameter vector θ comprises the learnable parameters of the VP layer. According to [21], the gradients of the VP operators can be directly calculated, and thus the backpropagation of the VP layer can be done in a natural way discussed in Section 2.3.

The properties and advantages of VPNet are the following:

- *Role*: A novel model-driven network architecture for 1D signal processing problems.
- *Generality*: VPNet can be built by arbitrary parameterized function systems, allowing the direct incorporation of the domain knowledge into the network.
- *Interpretability*: The VP layer can be explained as a built-in feature extraction method. Moreover, the layer parameters are the nonlinear VP system parameters that provide an interpretable meaning to them. They are usually directly connected to morphological properties of the input data (see e.g. Section 3.2).
- *Simplicity*: The VP layer is usually driven by a few system parameters only, thus VPNet may provide a compact alternative to CNNs and DNNs. Actually, the VP layer can significantly decrease the number of parameters in a DNN.

2.3 VP Backpropagation

Let us discuss the offline training of a general feedforward NN in a supervised manner. Let

$$(x_i, y_i) \quad (i = 1, 2, \dots, M)$$

be the annotated input-target pairs of the training data, where the input vector $x_i \in \mathbb{R}^m$ and the target vector $y_i \in \mathbb{R}^s$ (in case of regression) or the target label $y_i \in \mathbb{N}$ (in case of classification). A general feedforward NN can be expressed as the composition of layer functions of the form

$$NN_{\theta}(x) = \left(f_{\theta^{(L)}}^{(L)} \circ \dots \circ f_{\theta^{(\ell)}}^{(\ell)} \circ \dots \circ f_{\theta^{(2)}}^{(2)} \circ f_{\theta^{(1)}}^{(1)} \right) (x) \quad (x \in \mathbb{R}^m),$$

where $f_{\theta^{(\ell)}}^{(\ell)}$ and $\theta^{(\ell)}$ denote the function and parameters of layer ℓ , respectively. The symbol θ refers to set of parameters $\theta^{(\ell)}$. The layer functions $f^{(\ell)}$ may refer to linear mappings, convolutional filters, nonlinear activations, pooling, VP operators, etc. Let

$$\hat{y}_i := NN_{\theta}(x_i) \quad (i = 1, 2, \dots, M)$$

denote the predicted values for each input. The training of the network can be addressed as a minimization problem, involving a proper loss (i.e. cost) function J that evaluates the error between the predicted and target values. Common loss functions are the Mean Squared Error (MSE), i.e. the least squares cost function (regression problems, $y_i \in \mathbb{R}^s$), and the Binary Cross Entropy (BCE) loss (binary classification, $y_k \in \{0, 1\}$):

$$J_{MSE}(\theta) := \frac{1}{M} \sum_{i=1}^M \|y_i - \hat{y}_i\|_2^2, \quad J_{BCE}(\theta) := -\frac{1}{M} \sum_{i=1}^M (y_i \log \hat{y}_i + (1 - y_i) \log(1 - \hat{y}_i)).$$

In our experiments, we will utilize the Cross Entropy loss J_{CE} that is the multi-class extension of BCE (classification, $y_k \in \mathbb{N}$), see also Section 3.

The state-of-the-art method to train feedforward networks is the backpropagation that minimizes J by means of a stochastic gradient descent optimization. The gradient descent update formula for each layer parameter is

$$\theta^{(\ell)} := \theta^{(\ell)} - \varepsilon \frac{\partial J}{\partial \theta^{(\ell)}},$$

where $\varepsilon > 0$ is called the learning rate. Briefly, backpropagation provides a recursive way to compute the gradients above based on the chain rule:

$$\frac{\partial J}{\partial f^{(\ell-1)}} = \frac{\partial J}{\partial f^{(\ell)}} \cdot \frac{\partial f^{(\ell)}}{\partial f^{(\ell-1)}}, \quad \frac{\partial J}{\partial \theta^{(\ell)}} = \frac{\partial J}{\partial f^{(\ell)}} \cdot \frac{\partial f^{(\ell)}}{\partial \theta^{(\ell)}}.$$

This way, only the partial derivatives of the layer function $f^{(\ell)}$ with respect to its input ($\partial f^{(\ell)} / \partial f^{(\ell-1)}$) and to its parameters ($\partial f^{(\ell)} / \partial \theta^{(\ell)}$) need to be calculated. These derivatives are usually well-known for the common layer types, and can be directly calculated for the VP layers as well. Based on [21], the partial derivatives of the VP operators with respect to their input and nonlinear parameters can be expressed as follows. In case of a filtering type VP layer (see Eq. (4)):

$$f^{(\text{vp})}(x) = \Phi(\theta)\Phi^+(\theta)x, \quad \frac{\partial f^{(\text{vp})}}{\partial x} = [\Phi(\theta)\Phi^+(\theta)]^T, \quad \frac{\partial f^{(\text{vp})}}{\partial \theta_j} = \frac{\partial [\Phi(\theta)\Phi^+(\theta)]}{\partial \theta_j}x,$$

where

$$\partial [\Phi(\theta)\Phi^+(\theta)] = (I - \Phi\Phi^+)\partial\Phi\Phi^+ + [(I - \Phi\Phi^+)\partial\Phi\Phi^+]^T.$$

In case of a feature extraction type VP layer (see Eq. (5)):

$$f^{(\text{vp})}(x) = \Phi^+(\theta)x, \quad \frac{\partial f^{(\text{vp})}}{\partial x} = [\Phi^+(\theta)]^T, \quad \frac{\partial f^{(\text{vp})}}{\partial \theta_j} = \frac{\partial \Phi^+}{\partial \theta_j}x,$$

where

$$\partial\Phi^+ = -\Phi^+\partial\Phi\Phi^+ + \Phi^+ [\Phi^+]^T \partial\Phi^T (I - \Phi\Phi^+) + (I - \Phi^+\Phi)\partial\Phi^T [\Phi^+]^T \Phi^+.$$

The naive implementation of the backpropagation, particularly in case of DNNs, can lead to numerical issues, like divergence and overfitting. In order to avoid this, a regularization term, in form of an ℓ_2 penalty on the weight parameters, is added to the loss [33]. Here we introduce a percent root mean square difference (PRD) regularization that can be applied to a single feature extraction VP layer in case of a classification problem. The proposed modification of the loss function is

$$J_{VP}(\theta) := J_{CE}(\theta) + \frac{\alpha}{M} \sum_{i=1}^M \frac{\|x_i - \Phi(\theta^{(\text{vp})})\Phi^+(\theta^{(\text{vp})})x_i\|_2^2}{\|x_i\|_2^2} = J_{CE}(\theta) + \frac{\alpha}{M} \sum_{i=1}^M \frac{r_2(x_i; \theta^{(\text{vp})})}{\|x_i\|_2^2},$$

where $\alpha \geq 0$ controls the penalty effect. The motivation behind this regularization is twofold. First, it comes from the previous results that incorporate VP as feature extraction. This results show that the precise VP approximation may lead to 'good' features, and therefore to high classification accuracy. Second, we expect that the optimal VPNet classifier extract the main characteristics of the input signals, i.e. we presume 'good' approximation. This penalty term seemingly breaks the formulation of the backpropagation, but the original method can be easily extended by a bypass step that is applied to the VP layer only. The gradient with respect to the VP parameters are modified as follows:

$$\frac{\partial J_{VP}}{\partial \theta^{(\text{vp})}} = \frac{\partial J_{CE}}{\partial \theta^{(\text{vp})}} + \frac{\alpha}{M} \sum_{i=1}^M \frac{1}{\|x_i\|_2^2} \cdot \frac{\partial r_2}{\partial \theta^{(\text{vp})}},$$

where

$$\partial r_2 = -2x_i^T (I - \Phi\Phi^+) \partial\Phi\Phi^+ x_i.$$

3 Experiments

VPNet is evaluated and compared to fully-connected and 1D convolutional networks in supervised classification problems, motivated by particular biomedical signal processing applications. In the following we present the details of the experiments, such as the network architectures, the VP system of choice, and the synthetic and real datasets.

3.1 Network Architecture

Here we provide details about the networks we compared, the learning methods, and the network parameters. The networks are feedforward, consisting of the following layers:

- *VPNet*: a VP layer, a fully-connected (FC) layer with ReLU activation, an FC layer with SoftMax activation.
- *Fully-connected NN*: one or two FC layer with ReLU, an FC layer with SoftMax.
- *CNN*: a 1D convolutional and pooling layer, an FC layer with ReLU, an FC layer with SoftMax.

Designed for signal classification tasks, the inputs are \mathbb{R}^m samples, and the outputs are posterior probabilities with respect to the classes. The FC layers perform linear mappings with nonlinear activation (ReLU or SoftMax). The VP layer is a feature extraction type (see Eq. (5)), and the CNN implements 1D convolution and mean or maximum pooling, as in [10].

Offline backpropagation with Adam optimizer [34] was adopted as learning method, based on cross entropy loss with VP regularization (see Section 2.3). The hyperparameters and the parameter selection strategies are as follows:

- *Learning parameters*: learning rate, VP penalty (VPNet only), batch size, and the number of epochs. The latter two are fixed (512 and 10-100, respectively). The optimal learning rate and penalty can be selected by a grid search.
- *Network parameters*: number of layers, number of neurons, VP dimension n (VPNet only), convolutional and pooling kernel sizes (CNN only). Here we either used fix dimensions so that the three architectures are comparable, or evaluated possible configurations by a grid search.
- *Layer parameters*: linear weights and biases, nonlinear VP parameters (VPNet only), kernel weights and biases (CNN only). These parameters are optimized by the backpropagation. The initialization is random for the linear and kernel parameters. However, the VP parameters have interpretable meaning, which may lead to special initialization. We investigated two options: a grid search on the intervals of possible values, and the initialization by means of the best approximation.

3.2 Adaptive Hermite System

Although Hermite functions have shown a great potential in many fields such as molecular biology [35], computed tomography [36], radar [37], and physical optics [38], their main application area is 1D biomedical signal processing. The shape features of Hermite functions are well suited to model compactly supported waveforms such as spikes [39–43], which explains our motivation to use them in ECG heartbeat classification.

Let us consider the Hermite polynomials [44], which are defined by the three-term recurrence relation:

$$H_{k+1}(t) = 2tH_k(t) - 2kH_{k-1}(t) \quad (k \in \mathbb{N}^+, t \in \mathbb{R}),$$

where $H_0(t) = 1$ and $H_1(t) = 2t$. Then, the adaptive Hermite functions can be defined as follows:

$$\Phi_k(t, \tau, \lambda) = \sqrt{\lambda} \Phi_k(\lambda(t - \tau)), \quad \text{where} \quad \Phi_k(t) = H_k(t) e^{-t^2/2} / \sqrt{\pi^{1/2} 2^k k!} \quad (k \in \mathbb{N}^+).$$

For a given parameter value $\theta = (\tau, \lambda)$, the k th column of the matrix $\Phi(\theta)$ in Eq. (3) is defined by the values of k th adaptive Hermite function evaluated at some predefined points t_0, t_1, \dots, t_{m-1} . In case of proper discretization [45], the columns of $\Phi(\theta)$ are pairwise orthogonal and unit vectors for all θ , therefore, $\Phi^+(\theta) = \Phi^T(\theta)$, which heavily speeds up the computation of the VP gradient.

The nonlinear parameters τ and λ represent the time shift and the width of the modeled waveforms, respectively. Thus, the network learns the positions and the shapes of those waves/spikes which separate one class from another. For instance, in electrocardiography, a heartbeat signal comprises three individual waveforms, i.e. the QRS, T, P waves, which represent different phases of the cardiac cycle, and their properties are directly used by medical experts to make diagnosis. These features are learned by the VP layer, i.e. the amplitude and shape information is extracted by the linear coefficients c_k 's, while the position and width of the waves are captured by τ and λ . This approach is essentially different from CNN based methods, where there are no direct connections between the learned and the medical descriptors.

3.3 Synthetic Data

Our goal was to synthesize a dataset where we know the actual structure of the data depending on the generator parameters. On the other hand, we aimed to generate a dataset that has practical relevance, i.e. it is somehow related to actual signal processing problems. The generator system of choice is the adaptive Hermite system, which seems to fulfill these expectations, based on its applications in signal processing (see Section 3.2). The principles we followed to generate the dataset are discussed below.

Let us consider a general signal model by means of a linear combination of adaptive Hermite function of the form

$$x_i = \Phi(\tau_i, \lambda_i) \cdot c^{(i)} = \sum_{k=0}^{n-1} c_k^{(i)} \Phi_k(\tau_i, \lambda_i) \quad (i = 1, 2, \dots, M),$$

where (τ_i, λ_i) and $c^{(i)}$ refer to the sample-specific nonlinear parameters and coefficients, respectively. Based on the completeness of the Hermite system in $L^2(\mathbb{R})$, this formula provides a general approximation for arbitrary signals. However, the signal processing applications of VP and the Hermite system show that the proper selection of nonlinear parameters may lead to accurate low order approximations. The further investigation on this topic reveals that the nonlinear parameters

corresponds to coarse changes in the signal morphologies, while the coefficients reflect to fine details. For instance, we refer to [24], where the nonlinear parameters were utilized as global, patient-wise, and the coefficients as heartbeat-wised descriptors. Motivated by these aspects, we intended to construct a dataset where the nonlinear parameters are close to each other, and the coefficients form noticeably separable classes.

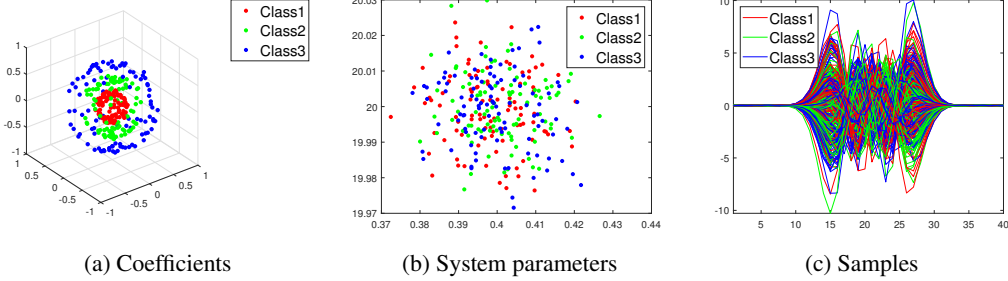


Figure 2: Synthetic dataset

More precisely, we considered five coefficients, i.e. $c^{(i)} \in \mathbb{R}^5$, so that the points $(c_1^{(i)}, c_2^{(i)}, c_3^{(i)}) \in \mathbb{R}^3$ form 3 separable spherical shells, which correspond to the target class labels (see Fig. 2 (a)). The motivation behind spherical shells is twofold. It is simple enough to support human interpretation, yet complicate enough to require complex networks. The last two coefficients, $c_4^{(i)}$ and $c_5^{(i)}$ serve as random factor as well as amplitude normalization. It is actually a misguidance to the classifier in the same time decreases the chance of overfitting. The nonlinear parameters τ_i and λ_i are similar for each sample up to a random factor, the sample-specific parameter values are generated randomly with given mean and variance (see Fig. 2 (b)). This factor simulates the nonlinear noise in the measurement. Fig. 2 (c) presents the samples themselves. We conclude that the simulation meets our expectations, i.e. the resulting samples are hard to separate, yet the underlying structure is easy to interpret.

In the actual implementation, 5000 samples per class were generated both for the training and test sets. We evaluated a total of more than 8000 possible hyperparameter configurations of the three network architectures. Namely, a range of neurons in the hidden layer, VP dimensions, CNN kernel and pooling sizes, learning rates, and VP initializations were considered. The VP penalty was preliminarily fixed to 0.1. The simulations show that the VP regularization can not only increase the learning speed but also can ensure convergence of an otherwise divergent configuration. In this regard, 0.1 is found to be a good choice. The aggregated results are presented in Fig. 3 (a) and (b). There, the configurations are grouped into six categories: VPNNets with dimension of $n = 7$ and 9 in Eq. (1), fully-connected NNs (FCNN), and CNNs with kernel size of 5, 15, and 25. Fig. 3 (a) displays the training accuracy curves corresponding to the best hyperparameter combination in each category. In Fig. 3 (b), the best test accuracies are plotted against the number of neurons in the hidden layer, for each category. Here, we would like to compare the performance of VPNet with respect to different network complexities.

The results demonstrate the efficiency and potential capabilities of VPNet. Fig. 3 (a) implies its fast learning ability. In fact, the convergence of VPNet is possibly faster than the other network architectures. Fig. 3 (b) proves that VPNet can potentially outperform FCNNs and CNNs with respect to the best accuracies on the test set. Although all architectures achieve accuracy close to 100%, VPNet provides these good results with low complexity. Here, low complexity refers not only to the number of neurons, but also to the total number of network parameters. In this regard, VPNet is

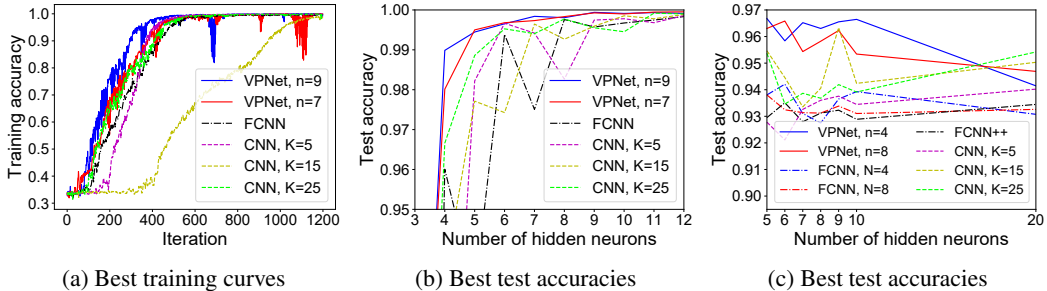


Figure 3: Evaluation on synthetic (a-b) and real data (c)

significantly better than the others. Namely, the number of parameters of FCNNs and CNNs, i.e. the linear and kernel weights and biases, exhibit linear growth with respect to the sample size and the number of neurons. Meanwhile, the number of nonlinear parameters ($p = 2$) of VPNet is independent of the sample size and output dimension.

3.4 Real ECG Data

Besides the simulations, we would like to prove the relevance of VPNet in a real signal processing problem, as well. In this respect, our choice is a particular ECG signal processing problem, the heartbeat arrhythmia classification (see [46]). The state-of-the-art is supervised ML by traditional approaches (see [11] and Section 1), including the VP-based static feature extraction [24, 31]. Here we do not aim to outperform these methods. Instead, we focus on a related subproblem, where we can compare the performance of the selected network configurations.

In more detail, we investigated the separation of the two largest arrhythmia classes, i.e. the normal and ventricular ectopic beats (VEBs). The source of the data is the benchmark MIT-BIH Arrhythmia Database [47], available of PhysioNet [48]. The database is split into sets DS1 and DS2 according to [49]. Although the whole database contains more than 100 000 annotated heartbeats, it is heavily biased towards the normal class. Here, a balanced subset was extracted: every VEB and the same number of normal beats from each record. That is 4260-4260 heartbeat signals for training (set DS1), and 3220-3220 signals for testing (set DS2). We note that the heartbeats of DS1 and DS2 come from different patients, i.e. there is no data leakage. We adopted the preprocessing and heartbeat extraction methods discussed in [31], with the exception that here the window size is selected to be 100 samples (~ 0.28 s) around the R peak annotations. This window is expected to cover the whole QRS complex and potentially the PR and ST segments of each heartbeat.

The performance of VPNet was measured in a similar way than in the synthetic case, with more than 3500 possible hyperparameter configurations examined. The aggregated results are presented in Fig. 3 (c). Here, the FCNN and CNN cases are restricted so that the output dimensions of the first layer are similar to the VP dimensions, and only the number of neurons in the hidden layer are varied. We note that VPNet has still remarkable lower number of network parameters. Besides, we evaluated another, larger FCNN configuration (FCNN++), where the number of neurons in the first layer is not restricted to the VP dimension n , instead it is the same as the number in the second, hidden layer. The structure and distribution of training and test data is more complex than in the synthetic case, which clearly makes the classification task more difficult for each network architecture. Again, we conclude that VPNet can potentially outperform FCNNs and CNNs for networks of low complexity.

4 Conclusion

We developed a novel model-driven NN which incorporates expert knowledge via variable projections. The VP layer is a generic, learnable feature extractor or filtering method that can be adjusted to several 1D signal processing problems by choosing an application specific function system. The proposed architecture is simple, i.e. it has only a few parameters, which are interpretable. Our case studies showed that the VPNet can achieve similar, or slightly better classification accuracy than its fully connected and CNN counterparts using less number of parameters. In our tests, the rate of convergence was approximately the same for the tested methods. However, the VP layer required only two parameters to learn in all cases, whereas the number of weights and biases for the FCNN and CNN grew linearly with the length of the input signals. Based on these results, we believe that VPNet can be effectively used for various problems in 1D signal processing including classification, regression, and even clustering problems. This will be part of future work.

Finally, we note that the construction of VPNet is general in nature, since the prior knowledge is incorporated via the basis functions Φ_k 's and their parameterization θ . Indeed, several applications can be reformulated as a VP problem [22]. For instance, the function system $\Phi_k(t, \tau_k, \lambda_k) = \cos(\lambda_k t + \tau_k)$ can be used in frequency estimation and in electroencephalography (EEG), where the network would learn dominant frequencies λ_k and phases τ_k that characterize a certain class of signals such as seizures in EEG recordings [50]. MRI imaging is another example [51], where $\Phi_k(t, \lambda_k) = \exp(\lambda_k t)$ with $\lambda_k \in \mathbb{R}^+$ yielding information about the tissue type. Therefore, the VPNet can be adjusted to several problems by choosing an application specific function systems and a proper parametrization.

Broader Impact

In this paper, the authors propose a new compact and interpretable neural network architecture that can have a broader impact in mainly two fields: machine learning and signal processing. The key idea is to create a network that combines the representation abilities of variable projections and the prediction abilities of NNs in form of a joint model. This concept can be generalized to other machine learning algorithms. For instance, VP-SVM, along with other combined VP methods, like VP-K-means and VP-C-means, can extend the potential area of applications, including classification and regression type, as well as clustering problems. Since the nonlinear parameters of the VP layer are interpretable, they can also be used in feature space augmentation, where new data is generated from existing ones in order to improve the generalization properties of DNNs [52, 53].

Signal processing aspects of the VPNet were discussed in the case study of ECG heartbeat classification. In addition to that, the VPNet can have a great potential in a wide range of applications especially where the VP has proven to be an efficient estimation method (cf. Section 3.2). Note that many already existing adaptive signal models were reformulated as a VP problem [22], however, parameterized wavelets [54] have not been studied yet in this context. Therefore, we encourage researchers to study this class of wavelets in the framework of VPNet.

Model-driven neural network solutions can have a great impact in biomedical engineering and health-care informatics, where the bare classification of medical data is usually not enough, physiological interpretation and explainability of the results are also important. However, these solutions should be applied in real world with a special care to avoid automation bias [55]. Justification of these clinical decision support systems is also difficult, since it requires both medical experts and a huge amount of data. The latter is naturally unbalanced in the sense that one class of signals, e.g. from normal patients, is over represented compared to the others. In order to mitigate these risks, VPNet should be tested in various scenarios including noisy and incomplete measurements, unbalanced data, etc.

References

- [1] J. Schmidhuber. Deep learning in neural networks: An overview. *Neural Networks*, 61:85–117, 2015. DOI: 10.1016/j.neunet.2014.09.003.
- [2] E. Alpaydin. *Introduction to Machine Learning*. Adaptive Computation and Machine Learning series. The MIT Press, 4th ed. edition, 2020. ISBN: 978-0262012430.
- [3] Y. Bengio, A. Courville, and P. Vincent. Representation Learning: A Review and New Perspectives. *IEEE Transactions on Pattern Analysis and Machine Intelligence*, 35(8):1798–1828, 2013. DOI: 10.1109/TPAMI.2013.50.
- [4] G. E. Hinton and R. R. Salakhutdinov. Reducing the dimensionality of data with neural networks. *Science*, 313(5786):504–507, 2006. DOI: 10.1126/science.1127647.
- [5] A. Krizhevsky, I. Sutskever, and G. E. Hinton. Imagenet classification with deep convolutional neural networks. In F. Pereira, C. J. C. Burges, L. Bottou, and K. Q. Weinberger, editors, *Advances in Neural Information Processing Systems 25*, pages 1097–1105. Curran Associates, Inc., 2012. DOI: 10.1145/3065386.
- [6] M. D. Zeiler and R. Fergus. Visualizing and understanding convolutional networks. In D. Fleet, T. Pajdla, B. Schiele, and T. Tuytelaars, editors, *Computer Vision – ECCV 2014*, pages 818–833, Cham, 2014. Springer International Publishing. DOI: 10.1007/978-3-319-10590-1_53.
- [7] C. Szegedy, W. Liu, Y. Jia, P. Sermanet, S. Reed, D. Anguelov, D. Erhan, V. Vanhoucke, and A. Rabinovich. Going deeper with convolutions. In *2015 IEEE Conference on Computer Vision and Pattern Recognition (CVPR)*, pages 1–9, 2015. DOI: 10.1109/CVPR.2015.7298594.
- [8] O. Ronneberger, P. Fischer, and T. Brox. U-net: Convolutional networks for biomedical image segmentation. In *International Conference on Medical image computing and computer-assisted intervention*, pages 234–241. Springer, 2015. DOI: 10.1007/978-3-319-24574-4_28.
- [9] H. He, S. Jin, Wen C.-K., F. Gao, Li G. Y., and Z. Xu. Model-driven deep learning for physical layer communications. *IEEE Wireless Communications*, 26(5):77–83, 2019. DOI: 10.1109/MWC.2019.1800447.

- [10] S. Kiranyaz, T. Ince, and M. Gabbouj. Real-time patient-specific ecg classification by 1-d convolutional neural networks. *IEEE Transactions on Biomedical Engineering*, 63(3):664–675, 2016. DOI: 10.1109/TBME.2015.2468589.
- [11] E. J. S. Luz, W. R. Schwartz, G. Cámara-Chávez, and D. Menotti. ECG-based heartbeat classification for arrhythmia detection: A survey. *Computer Methods and Programs in Biomedicine*, 127:144–164, 2016. DOI: 10.1016/j.cmpb.2015.12.008.
- [12] J. R. Hershey, J. Le Roux, and F. Weninger. Deep unfolding: Model-based inspiration of novel deep architectures, 2014. arXiv: 1409.2574.
- [13] H. Yu, J. Peng, and Y. Tang. Identification of nonlinear dynamic systems using Hammerstein-type neural network. *Mathematical Problems in Engineering*, 2014. DOI: 10.1155/2014/959507.
- [14] Ławrińczuk M. Practical nonlinear predictive control algorithms for neural Wiener models. *Journal of Process Control*, 23(5):696–714, 2013. DOI: 10.1016/j.jprocont.2013.02.004.
- [15] M. Borgerding, P. Schniter, and S. Rangan. AMP-inspired deep networks for sparse linear inverse problems. *IEEE Transactions on Signal Processing*, 65(16):4293–4308, 2017. DOI: 10.1109/TSP.2017.2708040.
- [16] D. Ito, S. Takabe, and T. Wadayama. Trainable ISTA for sparse signal recovery. *IEEE Transactions on Signal Processing*, 67(12):3113–3125, 2019. DOI: 10.1109/TSP.2019.2912879.
- [17] A. Balatsoukas-Stimming and C. Studer. Deep unfolding for communications systems: A survey and some new directions. In *2019 IEEE International Workshop on Signal Processing Systems (SiPS)*, pages 266–271, 2019. DOI: 10.1109/SiPS47522.2019.9020494.
- [18] A. T. Kristensen and A. Balatsoukas-Stimming A. Burg. Identification of non-linear RF systems using backpropagation, 2020. arXiv: 2001.09877.
- [19] S. Kiranyaz, O. Avci, O. Abdeljaber, T. Ince, M. Gabbouj, and D. J. Inman. 1D convolutional neural networks and applications: A survey, 2019. arXiv: 1905.03554.
- [20] P. Kovács, S. Fridli, and F. Schipp. Generalized rational variable projection with application in ECG compression. *IEEE Transactions on Signal Processing*, 68(16):478–492, 2020. DOI: 10.1109/TSP.2019.2961234.
- [21] G. H. Golub and V. Pereyra. The differentiation of pseudo-inverses and nonlinear least squares problems whose variables separate. *SIAM Journal on Numerical Analysis (SINUM)*, 10:413–432, 1973. DOI: 10.1137/0710036.
- [22] G. H. Golub and V. Pereyra. Separable nonlinear least squares: The variable projection method and its applications. *Inverse problems*, 19(2):R1–R26, 2003. DOI: 10.1088/0266-5611/19/2/201.
- [23] V. Pereyra, G. Scherer, and F. Wong. Variable projections neural network training. *Mathematics and Computers in Simulation*, 73(1):231–243, 2006. DOI: 10.1016/j.matcom.2006.06.017.
- [24] T. Dózsa, G. Bognár, and P. Kovács. Ensemble learning for heartbeat classification using adaptive orthogonal transformations. In R. Moreno-Díaz et al., editor, *Computer Aided Systems Theory—EUROCAST 2019: Part II*, volume 12014 of *LNCS*, pages 355–363. Springer, Cham, 2020. DOI: 10.1007/978-3-030-45096-0_44.
- [25] P. Kovács, C. Böck, J. Meier, and M. Huemer. ECG segmentation using adaptive Hermite functions. In *Proc. of the 51st Annual Asilomar Conference on Signals, Systems, and Computers*, pages 1476–1480, 2017. DOI: 10.1109/ACSSC.2017.8335601.
- [26] P. Kovács, C. Böck, T. Dózsa, J. Meier, and M. Huemer. Waveform modeling by adaptive weighted Hermite functions. In *Proc. of the 44th IEEE International Conference on Acoustics, Speech and Signal Processing (ICASSP)*, pages 1080–1084, 2019. DOI: 10.1109/ICASSP.2019.8683296.

- [27] S. Fridli, L. Lócsi, and F. Schipp. Rational function system in ECG processing. In R. Moreno-Díaz et al., editor, *Computer Aided Systems Theory–EUROCAST 2011: Part I*, volume 6927 of *LNCS*, pages 88–95. Springer-Verlag Berlin, Heidelberg, Germany, 2012. DOI: 10.1007/978-3-642-27549-4_12.
- [28] S. Fridli, P. Kovács, L. Lócsi, and F. Schipp. Rational modeling of multi-lead QRS complexes in ECG signals. *Annales Univ. Sci. Budapest., Sect. Comp.*, 37:145–155, 2012. URL: http://ac.inf.elte.hu/Vol_037_2012/145_37.pdf.
- [29] G. Bognár, S. Fridli, P. Kovács, and F. Schipp. Adaptive rational transformations in biomedical signal processing. In Simon Péter et al., editors, *Progress in Industrial Mathematics at ECMI 2018*, pages 239–247, Cham, 2019. Springer. DOI: 10.1007/978-3-030-27550-1_30.
- [30] K. Samiee, P. Kovács, and M. Gabbouj. Epileptic seizure classification of EEG time-series using rational discrete short time Fourier transform. *IEEE Transactions on Biomedical Engineering*, 62(2):541–552, 2014. DOI: 10.1109/TBME.2014.2360101.
- [31] G. Bognár and S. Fridli. Heartbeat classification of ECG signals using rational function systems. In R. Moreno-Díaz et al., editor, *Computer Aided Systems Theory–EUROCAST 2017: Part II*, volume 10672 of *LNCS*, pages 187–195. Springer, Cham, 2018. DOI: 10.1007/978-3-319-74727-9_22.
- [32] G. Bognár and S. Fridli. ECG segmentation by adaptive rational transform. In R. Moreno-Díaz et al., editor, *Computer Aided Systems Theory–EUROCAST 2019: Part II*, volume 12014 of *LNCS*, pages 347–354. Springer, Cham, 2020. DOI: 10.1007/978-3-030-45096-0_43.
- [33] I. Goodfellow, Y. Bengio, and A. Courville. *Deep Learning*. MIT Press, 2016. ISBN: 978-0262035613.
- [34] D. P. Kingma and J. Ba. Adam: A method for stochastic optimization, 2014. arXiv: 1412.6980.
- [35] G. Leibon, D. N. Rockmore, W. Park, R. Taintor, and G. S. Chirikjian. A fast Hermite transform. *Theoretical Computer Science*, 409(2):211–228, 2008. DOI: 10.1016/j.tcs.2008.09.010.
- [36] E. Moya-Albor, B. Escalante-Ramírez, and E. Vallejob. Optical flow estimation in cardiac CT images using the steered Hermite transform. *Signal Processing: Image Communication*, 28(3):267–291, 2013. DOI: 10.1016/j.image.2012.11.005.
- [37] S. Stanković, I. Orović, and A. Krylov. The two-dimensional Hermite S-method for high resolution inverse synthetic aperture radar imaging applications. *IET Signal Process*, 4(4):352–362, 2010. DOI: 10.1049/iet-spr.2009.0060.
- [38] P. Lazaridis, G. Debarge, and P. Gallion. Discrete orthogonal Gauss–Hermite transform for optical pulse propagation analysis. *Journal of the Optical Society of America B*, 20(7):1508–1513, 2003. DOI: 10.1364/JOSAB.20.001508.
- [39] L. R. Lo Conte, R. Merletti, and G. V. Sandri. Hermite expansions of compact support waveforms: Applications to myoelectric signals. *IEEE Transactions on Biomedical Engineering*, 41(12):1147–1159, 1994. DOI: 10.1109/10.335863.
- [40] M. Lagerholm, C. Peterson, G. Braccini, L. Edenbrandth, and L. Sörnmo. Clustering ECG complexes using Hermite functions and self-organizing maps. *IEEE Transactions on Biomedical Engineering*, 47:838–717, 2000. DOI: 10.1109/10.846677.
- [41] A. Sandryhaila, S. Saba, M. Püschel, and J. Kovacevic. Efficient compression of QRS complexes using Hermite expansion. *IEEE Transactions on Signal Processing*, 60(2):947–955, 2012. DOI: 10.1109/TSP.2011.2173336.
- [42] H. Haraldsson, L. Edenbrandt, and M. Ohlsson. Detecting acute myocardial infarction in the 12-lead ECG using Hermite expansions and neural networks. *Artificial Intelligence in Medicine*, 32:127–136, 2004. DOI: 10.1016/j.artmed.2004.01.003.
- [43] M. Brajović, I. Orović, M. Daković, and S. Stanković. On the parameterization of Hermite transform with application to the compression of QRS complexes. *Signal Processing*, 131:113–119, 2017. DOI: 10.1016/j.sigpro.2016.08.007.

- [44] G. Szegő. *Orthogonal polynomials*. AMS Colloquium Publications, New York, USA, 3rd edition, 1967. ISBN: 0-8218-1023-5.
- [45] W. Gautschi. *Orthogonal Polynomials, Computation and Approximation*. Numerical Mathematics and Scientific Computation. Oxford University Press, Oxford, UK, 2004. ISBN: 978-01-9850-672-0.
- [46] Association for the Advancement of Medical Instrumentation (AAMI). Testing and reporting performance results of cardiac rhythm and ST segment measurement algorithms. *American National Standards Institute (ANSI)*, ANSI/AAMI/ISO EC57, 1998-(R)2008.
- [47] G. B. Moody and R. G. Mark. The impact of the MIT-BIH Arrhythmia Database. *IEEE Eng. Med. Biol. Mag.*, 20(3):45–50, 5 2001. DOI: 10.1109/51.932724.
- [48] A. L. Goldberger et al. PhysioBank, PhysioToolkit, and PhysioNet: Components of a new research resource for complex physiologic signals. *Circulation*, 101(23):e215–e220, 6 2000. DOI: 10.1161/01.CIR.101.23.e215.
- [49] Philip de Chazal, M. O’Dwyer, and R. B. Reilly. Automatic classification of heartbeats using ECG morphology and heartbeat interval features. *IEEE Trans. Biomed. Eng.*, 51(7):1196–1206, 7 2004. DOI: 10.1109/TBME.2004.827359.
- [50] A. T. Tzallas, M. G. Tsipouras, and D. I. Fotiadis. Epileptic seizure detection in EEGs using time-frequency analysis. *IEEE Transactions on Information Technology in Biomedicine*, 13(5):703–710, 2009. DOI: 10.1109/TITB.2009.2017939.
- [51] M. Paluszny, M. Lentini, M. Martin-Landrove, and Torres. Recovery of relaxation rates in MRI T2 weighted brain images via exponential fitting. In V. Pereyra and G. Scherer, editors, *Exponential Data Fitting and its Applications*, pages 52–70. Bentham Science, 2010. DOI: 10.2174/978160805048211001010052.
- [52] Y. Bengio, F. Bastien, A. Bergeron, N. Boulanger-Lewandowski, T. Breuel, Y. Chherawala, M. Cisse, M. Côté, D. Erhan, J. Eustache, X. Glorot, X. Muller, P. S. Lebeuf, R. Pascanu, S. Rifai, F. Savard, and G. Sicard. Deep learners benefit more from out-of-distribution examples. In *Proceedings of the 14th International Conference on Artificial Intelligence and Statistics*, pages 164–172, 2011.
- [53] T. DeVries and G. W. Taylor. Dataset augmentation in feature space. In *Proceedings of the International Conference on Learning Representations (ICLR) Workshop*, pages 1–12, 2017. URL: <http://proceedings.mlr.press/v15/bengio11b.html>.
- [54] C. S. Burrus, A. R. Gopinath, and H. Guo. *Introduction to Wavelets and Wavelet Transforms: A primer*, chapter 5. Prentice Hall, New Jersey, USA, 1st edition, 1997. ISBN: 978-0134896007.
- [55] K. Goddard, A. Roudsari, and J. C. Wyatt. Automation bias: a systematic review of frequency, effect mediators, and mitigators. *Journal of the American Medical Informatics Association*, 19(1):121–127, 2012. DOI: 10.1136/amiajnl-2011-000089.